Chapter 1
Complex Fluids and Rheometry in Microfluidics

Francisco J. Galindo-Rosales

Abstract Complex fluids are everywhere, literally, just need to look around you, or even closer, inside your own body. These fluids are named *complex* because when they flow, they do not hold a linear relationship between the rate of deformation and the stress tensors, and consequently the Newton's law of viscosity is not suitable for them. In this chapter, the importance of the performing a rheological characterization and choosing the right constitutive model is highlighted, in particular when flowing at microscale, where the elastic behavior of these complex fluids is enhanced even at very small Reynolds numbers. Additionally, the potential of microfluidics as a platform for performing rheological characterizations is tackled.

1.1 Introduction

If we could depict a spectrum of mechanical behaviours of materials (Fig. 1.1), on the left side we would find Elastic Solid Materials as such exhibiting a linear relationship between the deformation tensor and the stress tensor, i.e. following Hooke's law of elasticity; on the right side of that spectrum we would have the Newtonian Fluids, as those materials that exhibit a linear relationship between the rate of deformation tensor and the stress tensor under flow, i.e. they follow Newton's law of viscosity. Any other material with the ability to flow would be placed in between these two extreme boundaries and is susceptible to be considered a *complex fluid*. Rheology is a branch of science dedicated to the study of deformation and flow of matter, it deals with materials that are neither Hookenian nor Newtonian, meaning that complex fluids in general range from *soft solids* to *elastic liquids* [8, 51, 56].

Complex fluids can be classified either as field-passive or field-active materials, depending on whether they need of an external field (magnetic or electric) to trigger their rheological behaviour or if their non-linear flow behaviour is simply shown upon the application of an external load, respectively [38]. In this chapter, the attention

F.J. Galindo-Rosales (✉)
Centro de Estudos de Fenómenos de Transporte, Faculdade de Engenharia da Universidade do Porto, Rua Dr. Roberto Frias, S/n, CP 4220-465 Porto, Portugal
e-mail: galindo@fe.up.pt

F.J. Galindo-Rosales (ed.), *Complex Fluid-Flows in Microfluidics*,
DOI 10.1007/978-3-319-59593-1_1

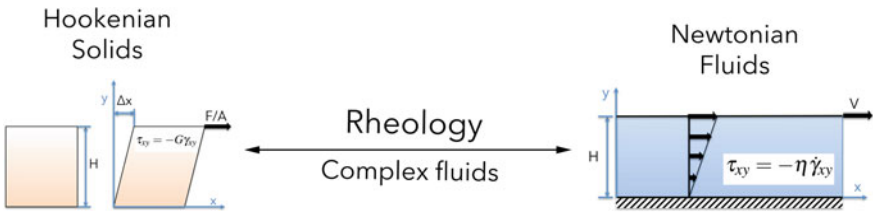

Fig. 1.1 Spectrum of mechanical behaviours of materials, ranging from Hookenian solids to Newtonian fluids. Rheology connects these two ideal mechanical behaviours and focus on the study of the deformation and flow of complex fluids, from soft solids to elastic liquids

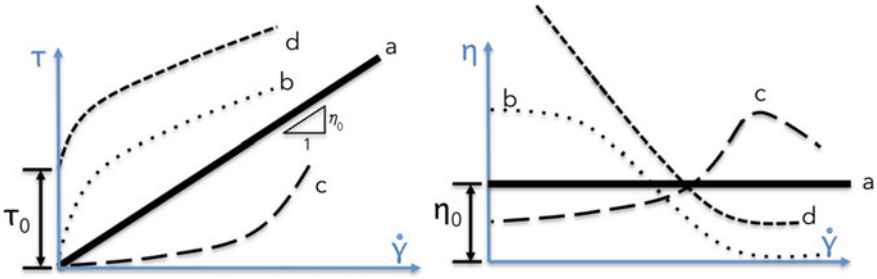

Fig. 1.2 Flow curve (*left*) and viscosity curve (*right*) of a Newtonian fluid **a** and three Generalized Newtonian Fluids: **b** Shear thinning fluid, **c** Shear thickening fluid, and **d** Yield Stress fluid

will be focused on field-passive materials, but readers interested in the rheological behaviour of field-active materials and their applications in microfluidics can find more information in the reviews of Sheng [67] and Nguyen [58]. A classical example of field-passive complex fluid is the silly putty, which exhibits solid-like behavior when subjected to quick mechanical deformations, while it flows like a thick liquid when the time of deformation is rather large. Greek yogurt is another traditional example of a field-passive complex fluids behaving like a soft-solid at rest while flowing like a liquid under sufficiently large shear stresses.

Typically, the source of the non-linearity between stress and rate of deformation tensors in a complex fluid has to be found in its formulation, that is either in the presence of molecular chains or in the existence of aggregates of nanoparticles. The way in which they stretch, orient and even break due to the flow dynamics and how they relax upon the release of the stresses is responsible for the bulk rheological behaviour of the fluid. The rheological behavior serve to sort complex fluids into two major groups: Generalized Newtonian Fluids (GNF's) and Viscoelastic Fluids (VEFs). GNF's show a non-linear relationship between the shear stresses and the applied shear rates, given by their apparent viscosity, which is not a constant, but a function of the shear rate. The dependency of the apparent viscosity with the shear rate allows the definition of different rheological behaviours, i.e. shear thinning, shear thickening and yield stress (Fig. 1.2).

GNF's are always be considered as inelastic fluids. Only VEF's exhibit simultaneously properties of elastic solids and viscous liquids, and therefore a characteristic relaxation time (λ) [54].

That characteristic relaxation time is responsible for the definition of the two most representative dimensionless numbers in rheology [60]: the Deborah number, defined as the relationship between the relaxation time and the duration of the deformation ($De = \frac{\lambda}{T}$); and the Weissenberg number, defined as the relaxation time multiplied by the rate of deformation ($Wi = \frac{\lambda U}{L}$). While the Deborah number allows distinguishing between solid-like ($De \uparrow$) and liquid-like ($De \downarrow$)behaviors of a particular material experiencing a deformation over a given timeframe, the Weissenberg number represents the ratio of elastic to viscous forces when a complex fluids is under flow. In general, Deborah and the Weissenberg numbers are not equivalent and the Weissenberg number is the one representing the nonlinearity of the rheological response of a viscoelastic material [22]. Thus, the steady, incompressible isothermal flow of a viscoelastic fluid is fully defined by the Weissenberg number and the Reynolds number ($Re = \frac{\rho U L}{\eta}$), being the latter the ratio of the inertial to viscous forces. The ratio between them defines the Elasticity number ($El = \frac{Wi}{Re} = \frac{\lambda \eta}{\rho L^2}$), which represents the ratio of elastic to inertial forces in the flow of a viscoelastic fluid [70].

Even for fluids with small relaxation times, microfluidics allows the exploration of zones in the Wi-Re parameter space unreachable at macroscale, due to the very small characteristic length scale that enhances the elastic effects ($L \downarrow \Rightarrow El \uparrow$) [65].

Additionally, for the same reason, elastic instabilities may be triggered with relative ease, an consequently the flow of viscoelastic fluids can be very different from their Newtonian and Generalized Newtonian counterparts [33]. This intrinsic capacity for enhancing the elastic behavior of the viscoelastic fluids at low Reynolds numbers makes of microfluidics an unrivalled platform for both (1) performing rheological characterization beyond the limits of the commercial rheometers at macroscale [32, 69], and (2) for designing microfluidic rectifiers, i.e. microchannels with anisotropic flow resistance so that they can operate as fluidic devices (flux stabilizer or bistable flip-flop memory) similar to their solid-state electronic counterparts [40, 41] or they can be used for optimizing the mechanical performance of reinforced composites [36, 37]. Additionally, elastic instabilities can also be exploited for mixing enhancement at low Reynolds numbers [39] and enhanced oil recovery applications [14, 31]. Moreover, microfluidics allows for isolating individual polymer molecules in precisely defined flows and assessing models for polymer dynamics [81].

In this chapter, the attention will be focus on the potential of microfluidics as a platform for performing rheometry of complex fluids.

1.2 Rheometry at Macroscale

Within the world of Rheology, the field of Rheometry deals with the experimental determination of the rheological properties of complex fluids. It is necessary to perform experimental tests under controlled deformations/stresses and flows and record the mechanical response of the sample. As it is done in other disciplines, such as solid mechanics, these experiments must be performed according to some standards in order to measure some material functions, like the viscosity, and allow sharing and comparing that information either for quality control, for quantitative analysis or modeling [56]. Thus, rheometers are commercially available devices allowing to perform rheometry at macroscale imposing a small set of standard flows; namely, simple shear and extensional flows. Figure 1.3 summarizes the most common techniques to fully characterize rheologically complex fluids at macroscale, from low viscoelastic liquids to polymer melts. The reader interested in learning more about standard rheometry can get deeper through specialized books [10, 50, 51, 55, 56, 77].

Despite the correct use of the commercially available rheometers would allow getting a full rheological characterization of most of the complex fluids, in some cases it can be very challenging and we may find some limitations. Recently, R.H. Ewoldt and co-workers [26] thoroughly revised and summarized all these challenges and limitations associated to the shear rheometry at macroscale. Some of these limitations can be overcome by scaling down to microscale:

1. Instrument specifications. As any experimental device, rheometers are limited by their intrinsic measurable ranges of load and displacement. Many viscoelastic fluids exhibit relaxation times rather small ($\leq$1 ms) and, consequently, their viscoelastic stresses are small in laminar macroscale flows. Thus, it becomes very difficult to measure their material functions in a conventional rheometer ($El \ll 1$). As mentioned above, working at microscales may help on solving this limitation, due to the enhancement of the elastic effects ($El >> 1$) [69].

2. Volume sample. In many cases, mainly when dealing with biological fluids, the availability of samples may be limited to very small quantities. Working with rheometrical techniques in which the characteristic length scale is well below 1 mm would allow to reduce extremely the consumption of volume samples to perform the experiments ($\leq$1 μl) [46, 47], without detriment to the accuracy in the measurements.

3. Instrument inertia. When the complex fluid is very soft and the rheological characterization is time dependent, such as in oscillatory tests, instrument inertia artifacts may appear. Microrheology techniques, thanks to the low inertia of colloidal probe particles, allow performing measurement of the linear rheology up to megahertz frequencies [88].

4. Fluid inertia. The assumption of having simple shear flow can be transgressed due to fluid inertia. When characterizing under simple shear soft low-viscous materials, either in transient or steady state conditions, fluid inertia issues may arise. Ewoldt et al. [26] highlighted two major sources of errors in the rheological characterization due to the inertia of the fluid: in oscillatory tests, the combination of high frequencies and low viscoelastic modulus may lead to propagating waves from either viscous momentum diffusion or elastic shear waves or both; secondary flows, either by inertial instabilities or elastic instabilities, may be originated at high velocities. Both fluid inertia effects that mask the physics of interest can be mitigated by performing a rheological characterization at microscale [81] .

To fully describe the flow properties of a complex fluid we must complement shear with extensional rheometry. Despite the recognized importance, the rheological characterization under pure extensional flows has been traditionally less explored due to intrinsic difficulties associated with imposing shear-free conditions. Consequently, the development of instrumentation has been delayed compared to the shear rheometry and mainly focused on high-viscous materials, i.e. polymer melts. Despite the great advances in extensional rheometry of low-viscosity complex fluids during the last years [24, 78, 85], two different filament stretching methods are still dominating the market place (CaBER™and FiSER™). However, as in shear rheometry, some challenges and limitations arise when characterizing the rheological properties of complex fluids in extensional flow:

1. Gravitational forces. Gravitational forces my have undesirable influence on reliability of the measurements obtained in both filament stretching rheometers. Firstly, the interfacial forces due to the surface tension must be larger than the gravitational body forces in order to allow the fluid forming the required liquid bridge between the plates and perform the experiment adequately. Secondly, gravitational forces may pull down the fluid and break the symmetry of the filament during the experiment run, leading to misleading dataset [35]. In microfluidic flows gravitational body forces can be neglected, as the Bond number, establishing the relationship between gravitational body forces and surface tension, is intrinsically very small ($Bo = \frac{\rho L^2 g}{\sigma} \ll 1$) [69].

2. Inertial effects. Despite the CaBER device allows characterizing the extensional properties of viscoelastic liquids with lower viscosity and elasticity than the FiSER, and the combination of the Slow Retraction Method [12] with the use of high speed cameras and small plates [80] may improve the results, inertial effects can be unavoidable below critical limits in viscosity and elasticity [74]. As discussed above, inertial effects can be neglected in rheometry at microscale.

3. Evaporation. In both extensional rheometers, CaBER™and FiSER™, fluid samples enjoy of having free surfaces, which is positive in the sense of having zero parallel shear stresses (shear-free flow), but can be negative when dealing with fluids exhibiting rapid solvent evaporation [71]. In this latter case, the use of microfluidics avoid that practical disadvantage.

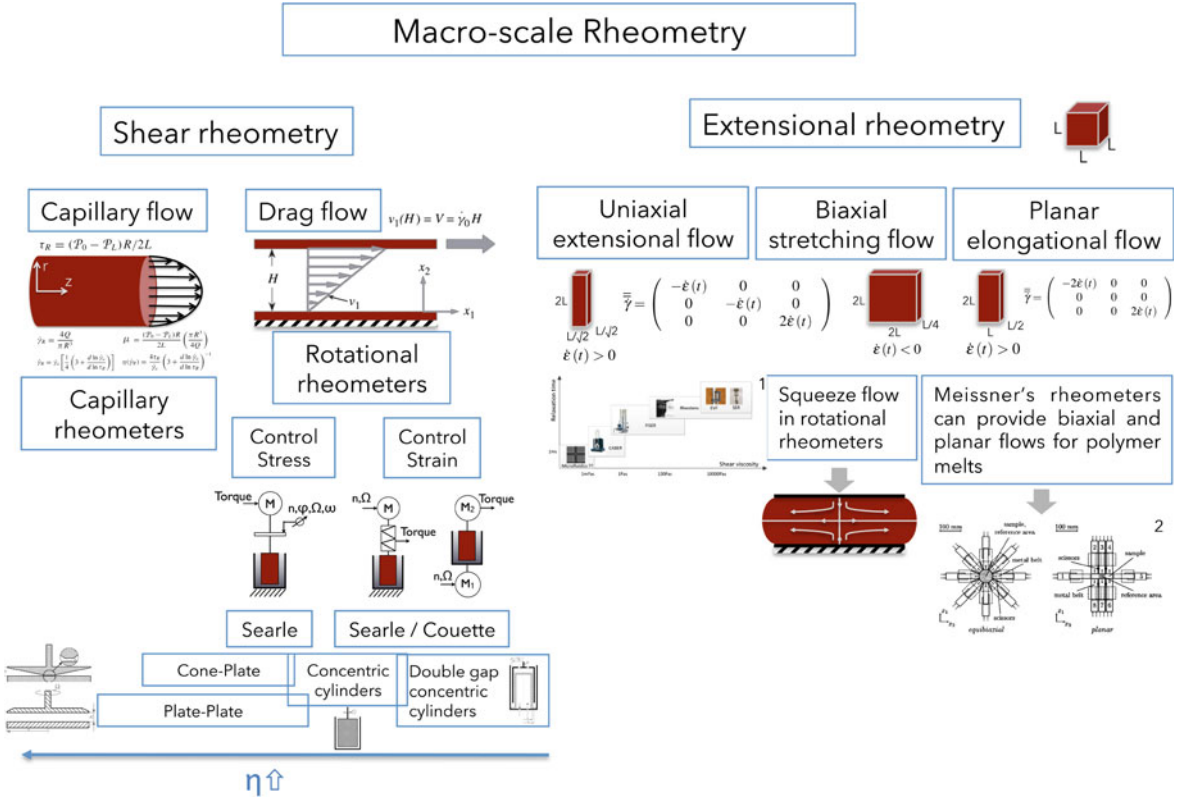

Fig. 1.3 Summary chart of the most common techniques to perform a rheological characterization at macroscale with commercial rheometers. The inset Fig. 1.1 showing the commercially available uniaxial extensional rheometers has been reproduced from Ref. [32] with permission of Springer. The inset Fig. 1.2 has been reprinted with permission from [44], Copyright 2003, The Society of Rheology

"Performing rheometry at microscale can solve many of limitations associated with standard rheometry at macroscale, particularly when working with complex fluids that are soft, have low-viscosity or are prone to evaporation."

1.3 Rheometry at Microscale

In the words of Clasen and McKinley [18] the term *microrheometry* "may be best defined as the science of measuring, quantitatively, the rheological properties of a fluid sample when one characteristic dimension is on the scale of order microns". They also proposed that the variety of different approaches to microrheometry can be sorted out into four major groups, graphically depicted in Fig. 1.4:

1. **Microrheology** allows the determination of the rheological properties of a complex fluid from the motion of probe particles embedded within it. Regarding the source of the force moving the probe particles, it can be distinguished passive microrheology, where particles move due to thermal energy [15, 53], from active microrheology, in which the probes are moved by optical or magnetic tweezers [73, 84]. These techniques are preferred for obtaining local and bulk shear viscoelastic properties both inside and outside the linear viscoelastic region. The reader interested in this topic can find more information in the following references [17, 21, 52, 82].

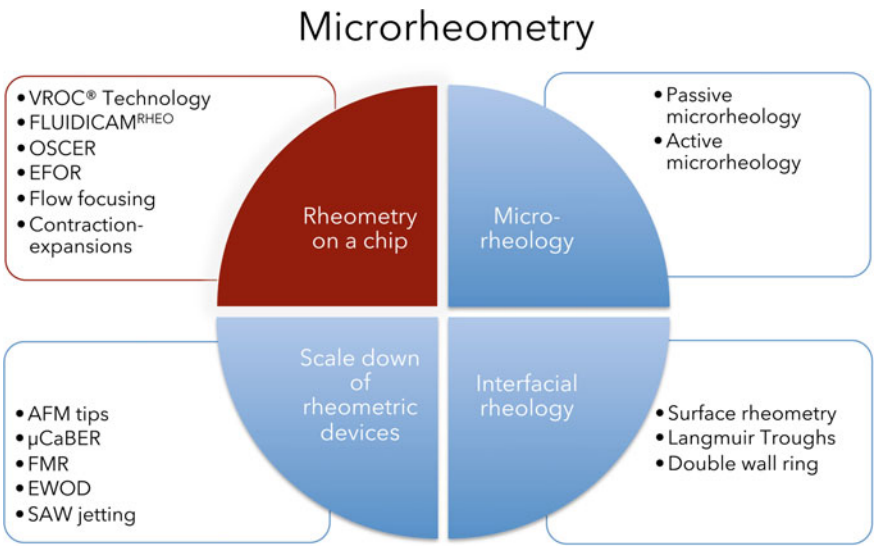

Fig. 1.4 Different approaches to microrheometry sorted out into four major groups

2. **Interfacial rheology** can be considered a kind of microrheometry, as it deals with the characterization of the static and dynamic properties of complex fluid-fluid interfaces, with one characteristic dimension on the scale of order of microns [18]. Complex fluid-fluid interfaces show nonlinear mechanical response to flow and deformation due to the presence of a microstructure, which can be originated by the presence of either surface-active molecules or micro/nano-particles at the interface. Further reading in this field of rheology is highly recommended through the review paper of Fuller and Vermant [28, 29] and their research works, such as [72, 76, 86, 87].

3. **Scale down of rheometric devices** can be of help for minimizing to gravitational and inertial effects inherent to low viscosity complex fluids. It can be found in the literature some examples able to extend the limits of reliable measurements compared with their macroscopic counterparts [9, 18, 25, 57, 80]. However, scaling down of some mechanical subsystems, mainly those including torsional motors, moving parts, and torque transducers may be impractical [69].

4. **Rheometry-on-a-chip** consists of characterizing the rheological properties of complex fluids in a microfluidic channel, under both standard rheometric flows (shear and extensional), and it has already proven great potential, particularly for low-viscosity complex fluids [32, 49, 69]. There are some intrinsic characteristics of microfluidics that turn it a great platform for rheometry: (a) Enhanced elastic behaviour of the fluid due to small length scale; (b) no evaporation issues; (c) small volume sample; (d) negligible inertial or gravitational effects; (e) the potentiality of producing highly integrated, portable and disposable/recyclable devices; (f) the possibility of optimizing numerically the geometry; (g) optical access and a direct characterization of the fluid-flow dynamics (see Chap. 3 for more details), measurement of velocity fields (particle tracking or micro-particle image velocimetry techniques) and stress tensors fields (birefringence technique); and (h) suitable to be used as an online rheological sensor in industrial processes. Hereafter attention will be devoted to the rheometry-on-a-chip approach, as highlighted in Fig. 1.4.

1.3.1 Shear Rheometry on a Chip

The development of rheometry-on-a-chip technology is following the steps of its macroscale counterpart. Firstly, all the efforts have been oriented towards performing steady state measurements, leading to a sufficient degree of matureness to reach the marketplace, as it is exemplified by VROC® technology and Fluidicam^{Rheo} device. The measurement of the viscoelastic moduli in rheometry-on-a-chip approach is yet scarce [16] and more work is required for the commercialization of a microdevice

able to provide viscoelastic moduli of complex fluids. At the current state of the art, these sort of characterization is preferred to be performed by microrheology (either active or passive).

> Current commercially available devices performing shear rheometry on a chip can only provide the apparent viscosity curve, that is the dependence of the viscosity with the imposed shear rate. If you are interested in characterizing the viscoelasticity in microscale, you are recommended to perform either passive or active microrheological experiments.

1.3.1.1 VROC® technology

The principle of VROC® technology [4, 68, 69] for performing shear rheometry on a chip (Fig. 1.5a) is based on the fundamentals of capillary rheometry at macroscale for a planar slit geometry, where the viscosity of the sample (η) is obtained from the steady fully developed flow condition by a relationship between the imposed flow rate (Q), the measured pressure drop (ΔP) along a capillary length (L) and a numerical factor (k) depending on the aspect ratio (width/depth, if $w/d >> 1$ then $k = 6$, while if $w/d = 1$ then $k = 14.3$) of the slit channel [69]. Equation 1.3 indicate that relationship for a laminar Newtonian flow in a planar slit geometry:

$$\tau_{wall} = \frac{wd}{2L\,(w+d)}\Delta P \tag{1.1}$$

$$\dot{\gamma}_{wall} = k\frac{Q}{wd^2} \tag{1.2}$$

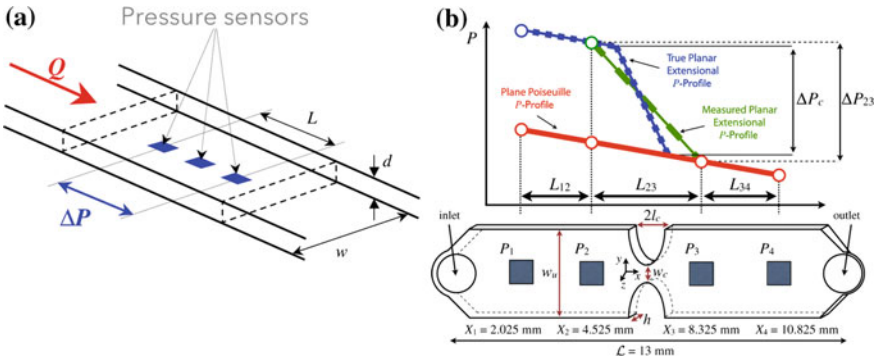

Fig. 1.5 Principle of the VROC® technology developed and commercialized by RheoSense. Reproduced from Ref. [59, 68] with permission of Springer

$$\eta = \frac{\tau_{wall}}{\dot{\gamma}_{wall}} = \frac{w^2 d^3}{2L\,(w+d)\,k}\frac{\Delta P}{Q}, \tag{1.3}$$

For fluids with a shear rate dependent viscosity, the Weissenberg-Rabinowitsch-Mooney correction for rectilinear channels is used to calculate the viscosity [51] and the viscosity is now given by the Eq. 1.7.

$$\tau_{wall} = \frac{wd}{2L\,(w+d)}\Delta P \tag{1.4}$$

$$\dot{\gamma}_{wall-app} = k\frac{Q}{wd^2} \tag{1.5}$$

$$\dot{\gamma}_{wall} = \dot{\gamma}_{wall-app}\frac{1}{3}\left[2 + \frac{dln\dot{\gamma}_{wall-app}}{dln\tau_{wall}}\right] \tag{1.6}$$

$$\eta = \frac{\tau_{wall}}{\dot{\gamma}_{wall}} = \frac{3w^2 d^3}{2L\,(w+d)\left[2 + \frac{dln\dot{\gamma}_{wall-app}}{dln\tau_{wall}}\right]k}\frac{\Delta P}{Q} \tag{1.7}$$

Flush mounted pressure transducers on the wide side of the channel provide direct measurement of the pressure gradient with negligible disturbance of the flow. The pressure transducer must be carefully calibrated to ensure accuracy in the measurements of viscosity over a wide shear rate range, at least an order of magnitude greater than in the standard macroscale rheometers [68]. RheoSense[1] is currently commercializing the VROC® technology, adapted for different samples, working temperatures, etc. The rectangular cross-section microchannel is made of glass and a Si low profile pressure sensor array is flush-mounted on one of the two wide sides. The equipments are provided with a software applications having implemented Eq. 1.7, in which the term $\frac{dln\dot{\gamma}_{wall-app}}{dln\tau_{wall}} = 1$ for Newtonian fluids and Eq. 1.7 then is equal to Eq. 1.3, while for non-Newtonian fluids $\frac{dln\dot{\gamma}_{wall-app}}{dln\tau_{wall}} \neq 1$.

Measuring accurately pressure drop in microfluidic devices is challenging (see Chap. 3 for further information). It can be found in the literature other approaches for measuring the pressure drop, such as the one proposed in [66] for PDMS microchannels. Nevertheless, the flush-mounted approach is probably a robust and adequate approach for a commercial rheometer-on-a-chip device.

VROC® Technology allows obtaining the viscosity curve of complex liquids (min volume 12 μl) with a shear viscosity ranging from 0.2 to 80,000 mPa·s under shear rates ranging from 0.5 to 1,000 s^{text-1}. Temperature control between 4 and 70 °C.

[1] http://www.rheosense.com Cited 30 April 2017.

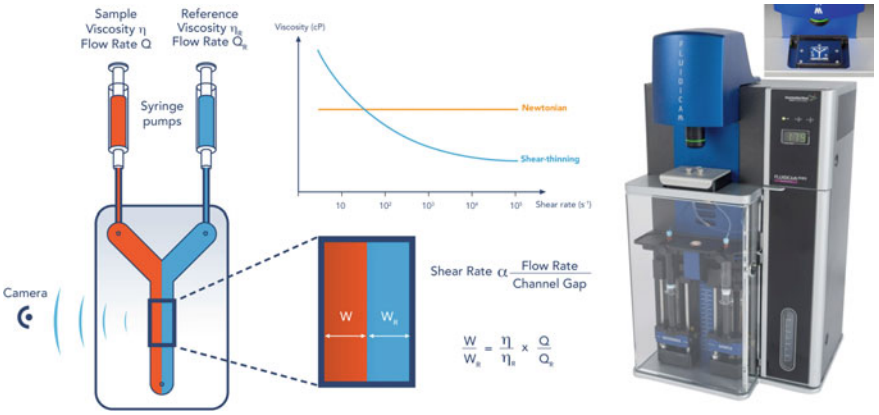

Fig. 1.6 Fluidicam$^{\text{Rheo}}$ device by formulaction. Reproduced from Ref. [27] with permission of Formulaction

1.3.1.2 Fluidicam$^{\text{Rheo}}$

The French company Formulaction[2] introduces Fluidicam$^{\text{Rheo}}$ in 2016 (Fig. 1.6), a microfluidic rheometer based on live imaging of a microfluidic co-flow. The technology was first demonstrated by Colin and co-workers [19, 42, 43], inspired by the work of Galambos and Foster [30].

The principle is straightforward: two fluids, the sample and a Newtonian reference fluid, flows together in a microfluidic channel. As the flow is laminar, a visible interface is formed between both fluids (miscible or not). Shear rate and sample viscosity is simply calculated from the knowledge of the reference viscosity, geometries of the fluid streams and flow rates. More precisely:

- Pressure gradient ∇P_r is calculated in the reference stream, knowing width W_r (measured with the camera), flow rate Q_r, viscosity η_r and channel depth h, using well established relationships [11], where suffixes r refer to the *reference fluid*. Considering $h \ll W_r$, pressure gradient can be written as $\nabla P_r = -\frac{12\eta_r}{h^3 W_r} Q_r$. More accurate models can also be used, better describing the flow in a rectangular cross section [75].
- Interface being straight, parallel to channel side walls, it is assumed that the pressure gradient in the sample stream equals the pressure gradient in the reference stream (otherwise there would be a visible transverse flow): $\nabla P = \nabla P_r$.
- Shear stress at the walls σ_w (up or bottom, separated by the channel depth h in Fig. 1.7) is calculated from the pressure gradient in the sample stream (balance between surface shear stresses and body pressure forces acting over a fluid element) [51]: $\sigma_w = -\frac{h}{2}\nabla P$.

[2] http://www.formulaction.com Cited 30 April 2017.

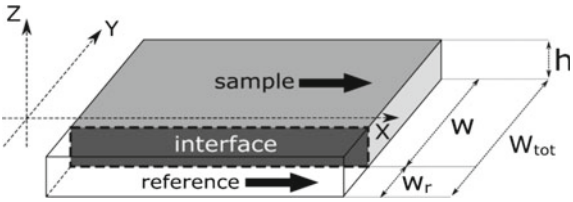

Fig. 1.7 Fluidicam^{Rheo} co-flow principle. Reproduced from Ref. [27] with permission of Formulaction

- Shear rate at the wall is calculated using the Rabinowitsch equation, independently from the rheological model: $\dot{\gamma}_w = \frac{2Q}{wh^2}\left[2 + \frac{dlnQ}{dln\sigma_w}\right]$.
- Finally, viscosity at the wall is calculated from its definition: $\eta_w = \frac{\sigma_w}{\dot{\gamma}_w}$.

In the original work from Colin et al. [19, 42, 43], the method involves manual settings of the flow rates until the interface is visible and located in a position suitable for measurement with a good accuracy. This step requires not only user attendance, but is also both time and sample consuming. Moreover, shear rates was not known before analysis, as it value depends on the interface position. This is an issue as most rheologists prefer to drive their viscosity measurements over a range of shear rates (representative of the end-user application) defined before the experiment, and not over a range of flow rates. Fluidicam^{Rheo} overcomes these issues with a user-friendly software built around a predictive control of the interface position, that allows to control experiments in term of shear rates (instead of flow rates), and a fully automated operation without user attendance. The instrument also integrates a fast temperature control from 4 to 80 °C. Finally, live imaging make understanding of rheological experiments much easier and comfortable, as it become possible to see the product flowing as the measurement is running.

Fluidicam^{Rheo} allows obtaining the viscosity curve of complex liquids (min volume 500 µl) with a shear viscosity ranging from 0.1 to 200,000 mPa·s under shear rates ranging from 100 to 100,000 s^{-1}. Temperature control between 4 and 80 °C.

1.3.1.3 Other Non-commercialized Approaches

Besides the approaches described in Sects. 1.3.1.1 and 1.3.1.2, there are many other approaches for performing shear rheometry on a chip that have not been commercialized yet. The following ones are innovative enough to deserve a mention here:

- **iCapillary-based viscometer**. Solomon et al. [79] recently proposed a new version of an image-based slit-microrheometer (Fig. 1.8). A constant pressure (P_c) is imposed at the inlet of a straight (L_{ch}) rectangular cross-section microchannel

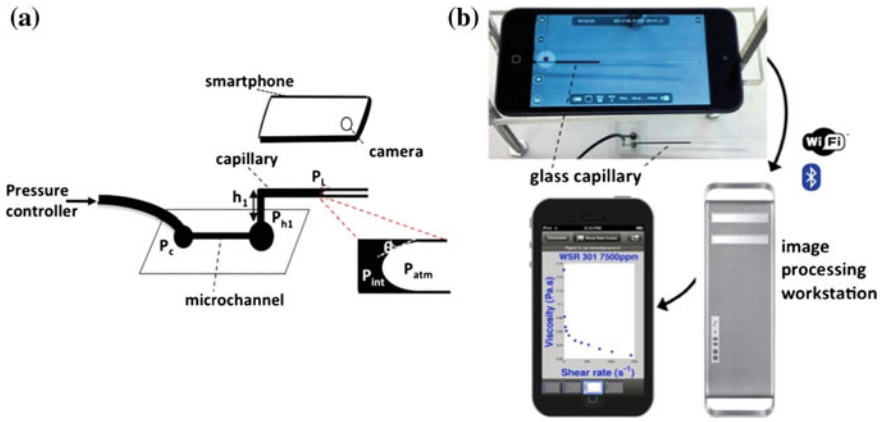

Fig. 1.8 Schematic and operation of the iCapillary-based viscometer. Reproduced from Ref. [79] with permission of Springer

($w >> h$). A L-shaped millimeter-scale glass capillary is connected at the outlet of the microchannel, having a vertical section h_1 providing a static head P_{h_1}. Thanks to the large diameter glass capillary, a smartphone camera can be used to record the motion of the interfacial meniscus and the capillary pressure due to the air-fluid interface is small compared to the driving pressure ($P_L = \frac{2\sigma cos\theta}{r}$). Thus, the wall shear stress is given by Eq. 1.8.

$$\tau_{wall} = \frac{\left(P_c - P_{h_1} + P_L\right) wh}{2L_{ch}\left(w + h\right)} \tag{1.8}$$

They also consider also Weissenberg-Rabinowitch-Mooney equation for determining the wall shear rate as a function of the flow rate. As the experiments are pressure driven, the flow rate is estimated by measuring the mean velocity of the meniscus (distance traveled over a period of time) and multiplying it by the cross-sectional area of the capillary. Thus, the viscosity is calculated for each imposed inlet pressure as $\eta = \frac{\tau_{wall}}{\dot{\gamma}_{wall}}$.

The main novelty of this approach lies on how τ_{wall} is calculated without using pressure sensors but controlling the pressure at the inlet and the outlet, and how the flow rate is calculated by means of an image analysis approach.

- **T-Junction microdevice**. While the measurement of a viscosity curve traditionally requires of multiple measurements, that is for every different point of the curve a different flow condition must be imposed, the approach proposed by Zimmerman and Ress [90] aims at improving the efficiency by obtaining the whole viscosity curve of a complex fluid in a single experiment. Inducing the flow field in such a microfludic channel either by an applied pressure drop or by an electric field (just

for electrokinetic flows), a range of shear rates can be generated within a single experiment due to the gradients on the characteristic velocity field associated with the flow in a T-junction. Bandalusena et al. [5–7] developed a procedure for assessing the total rheometric response for such a system based on the statistical moments of the velocity field (measured by means of μ-PIV technique) analysed in conjunction with finite element modelling. Despite the reliability of μ-PIV technique for providing the velocity field at microscale (Chap. 3), the equipment is expensive and bulky. Zimmerman et al. [89] showed numerically that it also exists a one-to-one mapping between the first three statistical moments of the end wall pressure profile with the parameters of the GNF models. The rheological curves can be also obtained from the pressure field in such a flow, which can be measured by means of piezoelectric pressure transducers in a more cost-effective way. Thus, from measurements from flow and pressure sensors in a microchannel T-junction, it is possible to solve the mathematically proscribed'inverse problem' in order to obtain the constitutive viscous parameters for GNF fluids. The addition of transient effects caused by pulsing of the fluid would allow to obtain the constitutive viscous parameters for viscoelastic fluids [90]. This latter feature is a step forward and major distinction regarding the previously described shear-rheometry-on-a-chip approaches.

Zimmerman and Ress approach would not only allow to obtain the constitutive viscous parameter for GNF fluids running just one experiment at steady flow conditions, but also the constitutive parameters for viscoelastic fluids under transient flow conditions.

1.3.2 Extensional Rheometry on a Chip

As in macroscale rheometry, despite the importance of characterizing the extensional properties of complex fluids, the development of experimental techniques at microscale for performing extensional flow tests has been delayed regarding the development of the shear techniques. To the best knowledge of the author, there is only one commercially available extensional rheometer-on-a-chip, based on VROC® technology.

1.3.2.1 EVROC™ viscometer

eVROC™ viscometer is based on Rheosense's patented VROC® technology [4], previously described in Sect. 1.3.1.1 for shear rheometry on a chip. In that case, the geometry microfluidic channel was straight and with a rectangular cross section, like

the macroscale counterpart for performing capillary experiments. That technology can be adapted for measuring both the shear and extensional viscosities simultaneously.

The chip used in eVROC™ has a hyperbolic contraction/expansion zone in the middle of the microchannel and four monolithically integrated MEMS pressure sensors symmetrically distributed upstream and downstream the contraction throat[3] (Fig. 1.5b). While abrupt contractions fail to produce homogeneous extension conditions [64], hyperbolically-shaped contraction in planar configurations allow to impose a strong extensional flow with an approximately constant extension rate along its centerline of the microchannel [13, 49, 59, 63], although there is an important contribution of the shear flow close to the lateral walls. This latter issue is the main reason why the eVROC™ microdevice includes four pressure sensors, for evaluating separately the pressure drop due to the viscous shear stresses (ΔP_v) in the fully developed regions (upstream and downstream the throat) and the pressure drop across the contraction/expansion zone (ΔP_c). By subtracting them, it would be possible to evaluate the pressure drop associated with the pure extensional flow ($\Delta P_e = \Delta P_c - \Delta P_v$) and resulting from the elastic normal stresses alone [59]. Thus, the apparent extensional viscosity for fully developed extensional flow in the hyperbolic contraction is given by Eq. 1.9:

$$\eta_{E,a} = \frac{1}{\varepsilon_H} \frac{\Delta P_e}{\dot{\varepsilon}_a}, \tag{1.9}$$

where $\dot{\varepsilon}_a = \frac{Q}{l_c h}\left(\frac{1}{w_c} - \frac{1}{w_u}\right)$ is the apparent extension rate, as a function of the flow rate (Q) and the geometrical parameters defining the hyperbolic contraction/expansion, and $\varepsilon_H = \int_0^t \dot{\varepsilon}_a dt'$ is the Hencky strain experience by a fluid element [59].

eVROC™ viscometer allows measuring the apparent extensional viscosity of complex liquids with a shear viscosity ranging from 20 to 2000 mPa·s under extension rates ranging from 0.1 to 1000 s^{-1}.

1.3.2.2 Other Non-commercialized Approaches

As in Sect. 1.3.1.3, there are also many other approaches in the literature for performing extensional rheometry on a chip that have not been commercialized yet. These alternative approaches look for technique able to overcome the major limitation of eVROC™ viscometer, which is the fact of having a region with combined shear and elongated characteristics in the flow kinematics [91]. The following ones are innovative enough to deserve a mention here:

[3] http://www.rheosense.com.

- **Optimized geometries**. In order to overcome the limitation of having a non-homogeneous velocity profile which results in a constant extension rate, Alves [1] developed an algorithm for optimal design of the geometry of the microchannel so that it provides the desired velocity field. That algorithm has been successfully implemented for different microfluidic devices, i.e. 2D [48] and 3D [34] cross-slots, hyperbolic contraction/expansion [34] and T-junction [2] providing uniform extension rates profiles. Figure 1.9 shows the optimization flowchart, a numerically optimized design, and the target velocity and strain-rate profiles along the centerline for a 3D optimized cross-slots geometry.

The combination of numerical flow simulations (see Chap. 4), numerical optimization techniques (see Chap. 5) and the experimental characterization fluid-flow dynamics (see Chap. 3) has been proven to provide excellent results for undergoing extensional rheometry on a chip.

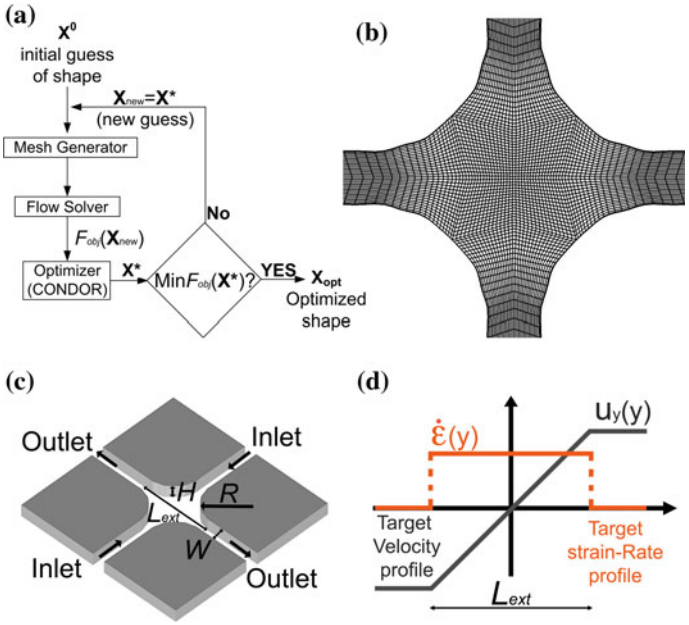

Fig. 1.9 Optimal shape design procedure. **a** Schematic illustration of the optimization flowchart, **b** top-view of an exemplifying optimized design and corresponding mesh, **c** 3D illustration of the optimized design including the geometric parameters, **d** target velocity and strain-rate profiles along the vertical centreline (x = 0). Reproduced from Ref. [34] with permission from The Royal Society of Chemistry

Working with these optimized geometries and the currently available experimental techniques for the characterization of the fluid-flow dynamics at microscale (see Chap. 3), it is possible to determine the extensional viscosity of low viscosity complex fluids accurately.

- **Particle migration**. Del Giudice et al. [23] proposed a completely different approach to determine the relaxation time of viscoelastic fluids (on the order of milliseconds) in a straight microfluidic channel, based on the viscoelasticity-induced particle migration phenomenon. The migration of a suspended particle in a flowing viscoelastic fluid towards the center of the microchannel is not due to inertia-driven migration effects, but instead it is governed by the dimensionless parameter $\theta = De\beta^2 \frac{L}{H}$, being L the distance from the inlet, H the depth of the channel and $\beta = D_p/H$ the confinement ratio of the particle with a diameter D_p. Recommended ranges for these two parameters are $H = 50 - 100$ μm and $\beta = 0.05 - 0.1$. Thus, by means of particle tracking experiments, it is calculated the particle distribution in the first band f_1 is calculated at different flow rates. Subsequently, θ is computed from f_1, and from that it is obtained the value of the Deborah number, providing the measurement of the fluid relaxation time. As θ is inversely proportional to H^4, very low relaxation times can be measured by using smaller channels, with a remarkable increase in the sensitivity of the measurements.

When performing rheometry on a chip, either under shear or extensional flow, it is important to adequately select the materials and the experimental tools. For instance, high pressures may deform the cross section of the PDMS microchannels produced by soft lithography techniques [45], endangering the reliability of the measurements and limiting the maximum values of shear rates or extension rates. In these cases, it is recommended the use of rigid materials (stainless steel, PMMA, fused silica, borosilicate glass, etc.) instead (see Chap. 2 for further information about the different fabrication techniques). Additionally, if the measurement of the pressure drop is relevant for the rheological characterization, it must be assessed if we should go for flush mounted or pressure taps (see Chap. 3 for further information about the different fluid-flow characterization techniques).

1.3.3 On-line Rheology Sensor: RheoStream®

One key aspect on industrial manufacturing of complex fluids (paints, food and beverages, pharmaceutical products, detergents, etc.) is monitoring the rheological properties of the fluid at different stages of the production in real time, so that the process operators and control systems can make decisions about their production. Traditionally, the viscosity was the fluid property measured on real time by means of different range of commercially available in-line viscometers. Nevertheless, as we already know, viscosity is not enough information when dealing with the process of complex fluids. Standard rheometry at macroscale can provide a full rheological

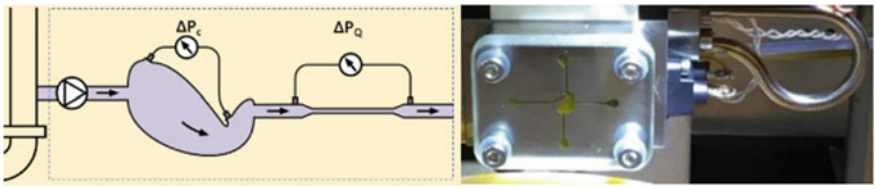

Fig. 1.10 RheoStream®, working principle (*left*) and a picture of the device (*right*). Reproduced with permission of Fluidan

characterization of these fluids in the laboratory, that is out-line of the production process. This implies a delay that disable the real-time control of the production process and that may result in a bottle neck in development, production and quality control. Thus, monitoring key rheological properties of complex fluids in-line the production process is crucial for manufacturing non-Newtonian fluids.

The RheoStream® device is commercialized by Fluidan[4] and can provide real-time continuous key rheological parameters in a given product or process. This technology combines capillary viscometry with a topologically optimized flow cell in which the rheological properties are related with differential pressure generated by the fluid-flow through it (Fig. 1.10) [61, 62]. The fundamental idea is that the total pressure drop measured in the optimized cell (ΔP_c) is the sum of two contributions: (1) the viscous contribution ($\Delta P_{c,V}$), which can be inferred from the capillary measurement ($\Delta P_{c,V} \propto \Delta P_Q$); and (2) the viscoelastic one ($\Delta P_{VE} = \Delta P_c - \Delta P_{c,V}$), which is calculated. The first normal stress in the fluid is proportional to the viscoelastic contribution to the pressure drop in the cell ($N_1 = k_1 \Delta P_{VE}$) [3] and N_1 can be correlated to the elastic modulus (G') by means of the extended Cox-Merz rule ($G' = C N_1^{\alpha} \dot{\gamma}_c^{2(1-\alpha)}$) [83], where C and α are calibration constant that must be determined for each working fluid, and $\dot{\gamma}_c$ is the characteristic shear rate in the flow cell that is correlated to the frequency in the oscillatory measurement performed in a rotational rheometer. Once the elastic modulus is obtained, the viscous modulus can be calculated ($G'' = \sqrt{G^{*2} - G'^2}$), where G^* is the complex modulus estimated from rescaling the shear stress (σ) by applying Cox-Merz rule [20].

The true power of RheoStream® is providing in-line real-time rheological parameters of complex fluids. Nevertheless, these parameters are not measured from "first principle", as the instrument needs to be calibrated to the working fluid.

[4] http://www.fluidan.com Cited 30 April 2017.

1.4 Summary

In this chapter, the following 10 key remarks/tips have been provided:

#1 GNF's are always be considered as inelastic fluids. Only VEF's exhibit simultaneously properties of elastic solids and viscous liquids, and therefore a characteristic relaxation time (λ).

#2 Even for fluids with small relaxation times, microfluidics allows the exploration of zones in the Wi-Re parameter space unreachable at macroscale, due to the very small characteristic length scale that enhances the elastic effects ($L \downarrow \Rightarrow El \uparrow$).

#3 Performing rheometry at microscale can solve many of limitations associated with standard rheometry at macroscale, particularly when working with complex fluids that are soft, have low-viscosity or are prone to evaporation.

#4 Current commercially available devices performing shear rheometry on a chip can only provide the apparent viscosity curve, that is the dependence of the viscosity with the imposed shear rate. If you are interested in characterizing the viscoelasticity in microscale, you are recommended to perform either passive or active microrheological experiments.

#5 VROC® Technology allows obtaining the viscosity curve of complex liquids (min volume 12 μl) with a shear viscosity ranging from 0.2 to 80,000 mPa·s under shear rates ranging from 0.5 to 1,000 s^{-1}. Temperature control between 4 and 70 °C.

#6 Fluidicam^{Rheo} allows obtaining the viscosity curve of complex liquids (min volume 500 μl) with a shear viscosity ranging from 0.1 to 200,000 mPa·s under shear rates ranging from 100 to 100,000 s^{-1}. Temperature control between 4 and 80 °C.

#7 Zimmerman and Ress approach would not only allow to obtain the constitutive viscous parameter for GNF fluids running just one experiment at steady flow conditions, but also the constitutive parameters for viscoelastic fluids under transient flow conditions.

#8 eVROC^{TM} viscometer allows measuring the apparent extensional viscosity of complex liquids with a shear viscosity ranging from 20 to 2000 mPa·s under extension rates ranging from 0.1 to 1000 s^{-1}.

#9 The combination of numerical flow simulations, numerical optimization techniques and the experimental characterization fluid-flow dynamics has been proven to provide excellent results for undergoing extensional rheometry on a chip.

#10 The true power of RheoStream® is providing in-line real-time rheological parameters of complex fluids. Nevertheless, these parameters are not measured from "first principle", as the instrument needs to be calibrated to the working fluid.

Acknowledgements F.J. Galindo-Rosales would like to acknowledge the financial support from FCT, COMPETE and FEDER through grant IF/00190/2013 and project IF/00190/2013/CP1160/CT 0003. The author would also like to thank Formulaction and Fluidan for fruitful discussion about their products, and for graciously providing the pictures used in Figs. 1.6, 1.7, and 1.10, respectively.

References

1. Alves, M. A. (2008). Design of a Cross-Slot flow channel for extensional viscosity measurements. *AIP Conference Proceedings*, *1027*(1), 240–242.
2. Alves, M. A. (2011). Design of optimized microfluidic devices for viscoelastic fluid flow. Technical Proceedings of the 2011 NSTI Nanotechnology Conference and Expo. 2: 474–477.
3. Baird, D. G. (2008). First normal stress difference measurements for polymer melts at high shear rates in a slit-die using hole and exit pressure data. *Journal of Non-Newtonian Fluid Mechanics*, *148*, 13–23.
4. Baek, S. G. (2010). Micro rheometer for measuring flow viscosity and elasticity for micron sample volumes. US Patent 7,770,436.
5. Bandalusena, H. C. H., Zimmerman, W. C., & Rees, J. M. (2009). Microfluidic rheometry of a polymer solution by micron resolution particle image velocimetry: A model validation study. *Measurement Science and Technology*, *20*(11), 115404.
6. Bandulasena, H. C. H., Zimmerman, W. B., & Rees, J. M. (2010). Creeping flow analysis of an integrated microfluidic device for rheometry. *Journal of Non-Newtonian Fluid Mechanics*, *165*, 1302–1308.
7. Bandulasena, H. C. H., Zimmerman, W. B., & Rees, J. M. (2010). Rheometry of non-Newtonian polymer solution by microchannel pressure driven flow. *Applied Rheology*, *20*, 55608.
8. Barnes H. A., Hutton J. F., & Walters, K. (1993). An introduction to Rheology. Rheology Series (Vol. 3). Amsterdam: Elsevier Science Publishers B.V.
9. Bhattacharjee, P. K., McDonnell, A. G., Prabhakar, R., Yeo, L. Y., & Friend, J. (2011). Extensional flow of low-viscosity fluids in capillary bridges formed by pulsed surface acoustic wave jetting. *New Journal of Physics*, *13*, 023005.
10. Bird, R. B., Armstrong, R. C., & Hassager, O. (1987). Dynamics of polymer liquids. Volume 1 - Fluid mechanics (2 edn). New York: Wiley.
11. Bruus, H. (2007). Theoretical microfluidics. Oxford University Press.
12. Campo-Deaño, L., & Clasen, C. (2010). The slow retraction method (SRM) for the determination of ultra-short relaxation times in capillary breakup extensional rheometry experiments. *Journal of Non-Newtonian Fluid Mechanics*, *165*(2324), 16881699.
13. Campo-Deaño, L., Galindo-Rosales, F. J., Oliveira, M. S. N., Alves, M. A., & Pinho, F. T. (2011). Flow of low viscosity boger fluids through a microfluidic hyperbolic contraction. *Journal of non-Newtonian Fluid Mechanics*, *166*(21–22), 1286–1296.
14. Campo-Deaño, L., Galindo-Rosales, F. J., Pinho, F. T., Alves, M. A., & Oliveira, M. S. N. (2012). Nanogel formation of polymer solutions flowing through porous media. *Soft Matter*, *8*(24), 6445–6453.
15. Campo-Deaño, L., Dullens, R. P. A., Aarts, D. G. A. L., Pinho, F. T., & Oliveira, M. S. N. (2013). Viscoelasticity of blood and viscoelastic blood analogues for use in polydymethylsiloxane in vitro models of the circulatory system. *Biomicrofluidics*, *7*, 034102.
16. Christopher, G. F., Yoo, J. M., Dagalakis, N., Hudson, S. D., & Migler, K. B. (2010). Development of a MEMS based dynamic rheometer. *Lab Chip*, *10*, 2749–2757.
17. Cicuta, P., & Donald, A. M. (2007). Microrheology: a review of the method and applications. *Soft Matter*, *3*, 1449–1455.
18. Clasen, C., & McKinley, G. H. (2004). Gap-dependent microrheometry of complex liquids. *Journal of non-Newtonian Fluid Mechanics*, *124*(1), 1–10.
19. Colin, A., Cristobal, G., Guillot, P., & Joanicot, M. (2012). Method and installation for determining rheological characteristics of a fluid, and corresponding identifying method. US Patent 8,104,329.
20. Cox, W. P., & Merz, E. H. (1958). Correlation of dynamic and steady flow viscosities. *Journal of Polymer Science*, *28*, 619–622.
21. Crocker, J. C., Valentine, M. T., Weeks, E. R., Gisler, T., Kaplan, P. D., Yodh, A. G., et al. (2000). Two-point microrheology of inhomogeneous soft materials. *Physical Review Letters*, *85*, 888.

22. Dealy, J. M. (2010). Weissenberg and deborah numbers their definition and use. *Rheology Bulletin (The Society of Rheology)*, *79*(2), 14–18.
23. Del Giudice, F., D'Avino, G., Greco, F., De Santo, I., Nettiab, P. A., & Maffettone, P. L. (2015). Rheometry-on-a-chip: measuring the relaxation time of a viscoelastic liquid through particle migration in microchannel flows. *Lab on a Chip*, *15*, 783–792.
24. Dinic, J., Zhang, Y., Jimenez, L. N., & Sharma, V. (2015). Extensional relaxation times of dilute, aqueous polymer solutions. *ACS Macro Letter*, *4*, 804808.
25. Erni, P., Varagnat, M., Clasen, C., Crest, J., & McKinley, G. H. (2011). Microrheometry of sub-nanolitre biopolymer samples: non-newtonian flow phenomena of carnivorous plant mucilage. *Soft Matter*, *7*, 10889.
26. Ewoldt, R. H., Johnston, M. T., & Caretta, L.M. (2015). Complex fluids in biological systems: experiment, theory, and computation. In: Spagnolie, S.E., (ed.) Chapter 6: experimental challenges of shear rheology: how to avoid bad data. New York: Springer.
27. Formulaction (2017). Fluidicam$^{\text{Rheo}}$ Technical specifications.
28. Fuller, G. G., & Verman, J. (2011). Editorial: dynamics and rheology of complex fluid-fluid interfaces. *Soft Matter*, *7*(17), 7583–7585.
29. Fuller, G. G., & Verman, J. (2012). Complex fluid-fluid interfaces: rheology and structure. *Annual Review of Chemical and Biomolecular Engineering*, *3*(1), 519–543.
30. Galambos, P., & Foster, F. (1998). An optical micro-fluidic viscometer. DSC-Vol. 66, Micro-Electro-Mechanicical System (MEMS). ASME International Mechanical Engineering Congress and Exposition, 15–20, Anaheim, CA.
31. Galindo-Rosales, F. J., Campo-Deaño, L., Pinho, F. T., van Bokhorst, E., Hamersma, P. J., Oliveira, M. S. N., et al. (2012). Microfluidic systems for the analysis of viscoelastic fluid flow phenomena in porous media. *Microfluidics and Nanofluidics*, *12*(1), 485–498.
32. Galindo-Rosales, F. J., Alves, M. A., & Oliveira, M. S. N. (2013). Microdevices for extensional rheometry of slow viscosity elastic liquids: a review. *Microfluidics Nanofluidics*, *14*, 1–19.
33. Galindo-Rosales, F. J., Campo-Deaño, L., Sousa, P. C., Ribeiro, V. M., Oliveira, M. S. N., Alves, M. A., et al. (2014). Viscoelastic instabilities in micro-scale flows. *Experimental Thermal and Fluid Science*, *59*, 128139.
34. Galindo-Rosales, F. J., Oliveira, M. S. N., & Alves, M. A. (2014). Optimized cross-slot microdevices for homogeneous extension. *RSC Advances*, *4*(15), 7799–7804.
35. Galindo-Rosales, F. J., Segovia-Gutirrez, J. P., Pinho, F. T., Alves, M. A., & de Vicente, J. (2015). Extensional rheometry of magnetic dispersions. *Journal of Rheology*, *59*(1), 193–209.
36. Galindo-Rosales, F. J., Martínez-Aranda, S., & Campo-Deaño, L. (2015). CorkSTFμfluidics - A novel concept for the development of eco-friendly light-weight energy absorbing composites. *Materials & Design*, *82*, 326–334.
37. Galindo-Rosales, F. J., & Campo-Deaño, L. (2016). Composite layer material for dampening external load, obtaining process, and uses thereof. WO Patent App. PCT/IB2015/057,399.
38. Galindo-Rosales, F. J. (2016). Complex fluids in energy dissipating systems. *Applied Sciences*, *6*(8), 206.
39. Groisman, A., & Steinberg, V. (2001). Efficient mixing at low Reynolds numbers using polymer additives. *Nature*, *410*, 905–908.
40. Groisman, A., Enzelberger, M., & Quake, S. R. (2003). Microfluidic memory and control devices. *Science*, *300*(5621), 955–958.
41. Groisman, A., & Quake, S. R. (2004). A microfluidic rectifier: anisotropic flow resistance at low reynolds numbers. *Physical Review Letters*, *92*(2), 094501.
42. Guillot, P., Panizza, P., Salmon, J.-B., Joanicot, M., & Colin, A. (2006). Viscosimeter on a microfluidic chip. *Langmuir*, *22*, 6438–6445.
43. Guillot, P., Moulin, T., Kotitz, R., Guirardel, M., Dodge, A., Joanicot, M., et al. (2008). Towards a continuous microfluidic rheometer. *Microfluidics Nanofluidics*, *5*, 619–630.
44. Hachmann, P., & Meissner, J. (2003). Rheometer for equibiaxial and planar elongations of polymer melts. *Journal of Rheology*, *47*(4), 989–1010.
45. Hardy, B. S., Uechi, K., Zhen, J., & Kavehpour, H. P. (2009). The deformation of flexible PDMS microchannels under a pressure driven flow. *Lab on a Chip*, *9*, 935–938.

46. Haward, S. J., Odell, J. A., Berry, M., & Hall, T. (2011). Extensional rheology of human saliva. *Rheologica Acta*, *50*(11), 869–879.
47. Haward, S. J., Sharma, V., & Odell, J. A. (2011). Extensional opto-rheometry with biofluids and ultra-dilute polymer solutions. *Soft Matter*, *7*(21), 9908–9921.
48. Haward, S. J., Oliveira, M. S. N., Alves, M. A., & McKinley, G. H. (2012). Optimized cross-slot flow geometry for microfluidic extensional rheometry. *Physical Review Letters*, *109*(12), 128301.
49. Haward, S. J. (2016). Microfluidic extensional rheometry using stagnation point flow. *Biomicrofluidics*, *10*(4), 043401.
50. Larson, R. G. (1999). *The structure and rheology of complex fluids*. New York, United States: Oxford University Press.
51. Macosko, C. W. (1994). *Rheology: principles, measurements, and applications*. United States: Wiley-VCH Inc.
52. Mason, T. G., & Weitz, D. A. (1995). Optical measurements of frequency-dependent linear viscoelastic moduli of complex fluids. *Physical Review Letters*, *74*, 1250.
53. Mason, T. G. (2000). Estimating the viscoelastic moduli of complex fluids using the generalized Stokes-Einstein equation. *Rheologica Acta*, *39*, 371–378.
54. Mewis, J., & Wagner, N. J. (2012). *Colloidal suspension rheology*. United Kindom: Cambridge University Press.
55. Mezger, T. G. (2002). The Rheology Handbook: for user of rotational and oscillatory rheometers. Vincentz Verlag, Germany.
56. Morrison, F. A. (2001). *Understanding rheology*. United States: Oxford University Press.
57. Nelson, W. C., Kavehpour, H. P., & Kim, C. J. (2011). A miniature capillary breakup extensional rheometer by electrostatically assisted generation of liquid filaments. *Lab Chip*, *11*, 2424–243.
58. Nguyen, N.-T. (2012). Micro-magnetofluidics: interactions between magnetism and fluid flow on the microscale. *Microfluidics and Nanofluidics*, *12*(1), 1–16.
59. Ober, T. J., Haward, S. J., Pipe, C. J., Soulages, J., & McKinley, G. H. (2013). Microfluidic extensional rheometry using a hyperbolic contraction geometry. *Rheologica Acta*, *52*(6), 529–546.
60. Official symbols and nomenclature of the society of rheology (2013). Journal of Rheology 57(4): 1047–1055.
61. Okkels, F. (2012). A flow measurement device and method. WO Patent App. PCT/DK2012/050,21.
62. Okkels, F., Oestergard, A.L., & Mohammadifar, M.A. (2017). Novel method for on-line rheology measurement in manufacturing of non-Newtonian liquids. Annual Transactions of the Nordic Rheology Society (Vol. 25).
63. Oliveira, M. S. N., Alves, M. A., Pinho, F. T., & McKinley, G. H. (2007). Viscous flow through microfabricated hyperbolic contractions. *Experiments in Fluids*, *43*(2–3), 437–451.
64. Oliveira, M. S. N., Rodd, L. E., McKinley, G. H., & Alves, M. A. (2008). Simulations of extensional flow in microrheometric devices. *Microfluidics and Nanofluidics*, *5*, 809–826.
65. Oliveira, M. S. N., Alves, M. A., & Pinho, F. T. (2011) Transport and mixing in laminar flows: from microfluidics to oceanic currents. Chapter 6: microfluidic flows of viscoelastic fluids. Wiley-VCH Verlag GmbH & Co. KGaA.
66. Pan, L., & Arratia, P. E. (2013). A high-shear, low Reynolds number microfluidic rheometer. *Microfluid Nanofluid*, *14*, 885894.
67. Sheng, P., & Wen, W. (2012). Electrorheological Fluids: Mechanisms, Dynamics, and Microfluidics Applications. *Annual Review Fluid Mechanics*, *44*, 14374.
68. Pipe, C., Majmudar, T. S., & McKinley, G. H. (2008). High shear rate viscometry. *Rheologica Acta*, *47*(5), 621–642.
69. Pipe, C., & McKinley, G. H. (2009). Microfluidic rheometry. *Mechanics Research Communications*, *36*, 110–120.
70. Poole, R. J. (2012). The Deborah and Weissenberg numbers. *British Society of Rheology, Rheology Bulletin*, *53*(2), 32–39.

71. Regev, O., Vandebril, S., Zussman, E., & Clasen, C. (2010). The role of interfacial viscoelasticity in the stabilization of an electrospun jet. *Polymer*, *51*, 2611–2620.
72. Reynaert, S., Brooks, C., Moldenaers, P., Vermant, J., & Fuller, G. G. (2008). Analysis of the magnetic rod interfacial stress rheometer. *Journal of Rheology*, *52*(1), 261–285.
73. Rich, J. P., Lammerding, J., McKinley, G. H., & Doyle, P. S. (2011). Nonlinear microrheology of an aging, yield stress fluid using magnetic tweezers. *Soft Matter*, *7*(21), 9933–9943.
74. Rodd, L. E., Scott, T. P., Cooper-White, J. J., & McKinley, G. H. (2005). Capillary break-up rheometry of low-viscosity elastic fluids. *Applied Rheology*, *15*, 1227.
75. Steinke, M. E., & Kandlikar, S. G. (2006). Single-phase liquid friction factors in microchannels. *International Journal of Thermal Sciences*, *45*, 1073–1083.
76. Samaniuk, J. R., & Vermant, J. (2014). Micro and macrorheology at fluid-fluid interfaces. *Soft Matter*, *10*(36), 7023–7033.
77. Schramm, G. (2000). *A practical approach to rheology and rheometry*. Karlsruhe, Germany: Haake GmbH.
78. Sharma, V., Haward, S. J., Serdy, J., Keshavarz, B., Soderlund, A., Threlfall-Holmes, P., et al. (2015). The rheology of aqueous solutions of ethyl hydroxy-ethyl cellulose (EHEC) and its hydrophobically modified analogue (hmEHEC): extensional flow response in capillary break-up, jetting (ROJER) and in a cross-slot extensional rheometer. *Soft Matter*, *11*, 32513270.
79. Solomon, D. E., Abdel-Raziq, A., & Vanapalli, S. A. (2016). *Rheologica Acta*, *55*(9), 727–738.
80. Sousa, P. C., Vega, E. J., Sousa, R. G., Montanero, J. M., & Alves, M. A. (2017). Measurement of relaxation times in extensional flow of weakly viscoelastic polymer solutions. *Rheologica Acta*, *56*(1), 1120.
81. Squires, T. M., & Quake, S. R. (2005). Microfluidics: Fluid physics at the nanoliter scale. *Reviews of Modern Physics*, *77*, 977–1026.
82. Squires, T. M., & Mason, T. G. (2010). Fluid Mechanics of Microrheology. *Annual Review of Fluid Mechanics*, *42*, 413–38.
83. Steffe, J. F. (1996). *Rheological methods in food engineering process* (2nd ed.). Press, East Lansing, USA: Freeman.
84. Tassieri, T., Del Giudice, F., Robertson, E. J., Jain, N., Fries, B., Wilson, R., et al. (2015). Microrheology with optical tweezers: Measuring the relative viscosity of solutions at a glance. *Scientific Reports*, *5*, 8831.
85. Vadillo, D. C., Tuladhar, T. R., Mulji, A. C., Mackley, M. R., Jung, S., & Hoath, S. D. (2010). The development of the 'Cambridge Trimaster' filament stretch and break-up device for the evaluation of ink jet fluids. *Journal of Rheology*, *54*(2), 261–282.
86. Vandebril, S., Franck, A., Fuller, G. G., Moldenaers, P., & Vermant, J. (2010). A double wall-ring geometry for interfacial shear rheometry. *Rheologica Acta*, *49*(2), 131–144.
87. Verwijlen, T., Leiske, D., Moldenaers, P., Vermant, J., & Fuller, G. G. (2012). Extensional rheometry at interfaces: Analysis of the Cambridge interfacial tensiometer. *Journal of Rheology*, *56*(5), 1225.
88. Waigh, T. A. (2005). Microrheology of complex fluids. *Reports on Progress in Physics*, *68*(3), 685.
89. Zimmerman, W. B., Rees, J. M., & Craven, T. J. (2006). The rheometry of non-Newtonian electrokinetic flow in a microchannel T-junction. *Microfluidics and Nanofluidics*, *2*, 481–492.
90. Zimmerman, W. C., & Rees, J. M. (2013). Rhemeter and rheometric method. WO Patent App. PCT/GB2013/051,089.
91. Zografos, K., Pimenta, F., Alves, M. A., & Oliveira, M. S. A. (2016). Microfluidic converging/diverging channels optimised for homogeneous extensional deformation. *Biomicrofluidics*, *10*, 043508.